

W^+W^- production at the LHC: NLO QCD corrections to the loop-induced gluon fusion channel

Massimiliano Grazzini^(a), Stefan Kallweit^(b),
Marius Wiesemann^(c) and Jeong Yeon Yook^(a)

^(a) Physik-Institut, Universität Zürich, 8057 Zürich, Switzerland

^(b) Dipartimento di Fisica, Università degli Studi di Milano-Bicocca and INFN, Sezione di
Milano-Bicocca, 20126, Milan, Italy

^(c) Max-Planck Institut für Physik, Föhringer Ring 6, 80805 München, Germany

Abstract

We compute the NLO QCD corrections to the loop-induced gluon fusion contribution in W^+W^- production at the LHC. We consider the full leptonic process $pp \rightarrow \ell^+\ell'^-\nu_\ell\bar{\nu}_{\ell'} + X$, by including resonant and non-resonant diagrams, spin correlations and off-shell effects. Quark–gluon partonic channels are included for the first time in the calculation, and our results are combined with NNLO predictions to the quark annihilation channel at the fully differential level. The computed corrections, which are formally of $\mathcal{O}(\alpha_s^2)$, increase the NNLO cross section by only about 2%, but have an impact on the shapes of kinematical distributions, in part due to the jet veto, which is usually applied to reduce the top-quark background. Our results, supplemented with NLO EW effects, provide the most advanced fixed-order predictions available to date for this process, and are compared with differential ATLAS data at $\sqrt{s} = 13$ TeV.

The production of vector-boson pairs plays a crucial role in precision studies at the Large Hadron Collider (LHC). Among the diboson processes, W -boson pair production has the largest cross section, and it provides direct access to the coupling between three electroweak (EW) vector bosons. This makes W^+W^- production ideal to test the gauge symmetry structure of EW interactions and the mechanism of EW symmetry breaking in the Standard Model (SM). It therefore provides an excellent probe of new-physics phenomena in indirect beyond-SM (BSM) searches [1–5]¹, and it was instrumental for the Higgs boson discovery [15, 16] as well as measurements of its properties [17–27].

The experimental precision of W^+W^- measurements is continuously increasing. Its cross section has been measured first in proton–anti-proton collisions at the Tevatron [28, 29], and later in proton–proton collisions at the LHC with centre-of-mass energies $\sqrt{s} = 7$ TeV [1, 2], 8 TeV [4, 5], and 13 TeV [30–32]. In particular, in the most recent 13 TeV measurement of Ref. [32] statistical uncertainties have already reached the few-percent level, even for distributions in the fiducial phase space. The systematic uncertainties are still comparably large, but they can be expected to further decrease in the future.

The increasing level of precision calls for continuous improvements in the theoretical description of W^+W^- production at hadron colliders. The experimental uncertainties can be matched on the theoretical side only by highest-order computations in QCD and EW perturbation theory. At leading order (LO) W -boson pairs are produced through quark annihilation, which was calculated for on-shell W bosons many years ago [33]. Next-to-leading-order (NLO) QCD predictions were first obtained in the on-shell approximation [34, 35], later incorporating leptonic W decays with off-shell effects and spin correlations [36–39]. To reach the precision demanded by present W^+W^- measurements, corrections beyond NLO QCD are indispensable. NLO EW corrections have been evaluated for on-shell W bosons [40–42], and with their full off-shell treatment [43–45]. Although EW effects have an impact of only few percent on the inclusive W^+W^- rate, they can be significantly enhanced up to several tens of percent at transverse momenta of about 1 TeV. At $\mathcal{O}(\alpha_s^2)$ the loop-induced gluon fusion channel provides a separately finite contribution, enhanced by the large gluon luminosity. This contribution, which is part of the next-to-next-to-leading order (NNLO) corrections, has been known for a long time [39, 46–55]. The complete NNLO QCD corrections were first evaluated in the on-shell approximation for the inclusive cross section [56], while the fully differential NNLO predictions for off-shell W bosons were presented in Ref. [57], using the two-loop helicity amplitudes for $q\bar{q} \rightarrow VV'$ [58–60]. Recently, the NLO QCD corrections to the loop-induced gluon fusion contribution, which are formally of $\mathcal{O}(\alpha_s^3)$, were evaluated [61] using the two-loop helicity amplitudes for $gg \rightarrow VV'$ of Refs. [62, 63], considering only the gluon–gluon partonic channel.

One important aspect of the theoretical description of W^+W^- production is the correct modelling of the jet veto (see Ref. [64–68] for example) that is applied in W^+W^- measurements to suppress the top-quark background. Studies based on resummed computations at next-to-next-to-leading logarithmic (NNLL) accuracy for the transverse momentum (p_T) of the W^+W^- pair [69] and for the jet-vetoed cross section [68] matched to NNLO, as well as the recent computation of Ref. [70] where NNLO predictions are matched to a parton shower, have shown that this is only relevant for small veto cuts. Jet vetos of 30 GeV and higher used in recent W^+W^- analyses [32] are sufficiently large to obtain reliable predictions for the fiducial cross section from fixed-order computations. On

¹See Refs. [6–14] as examples of theoretical ideas to exploit precision in diboson processes to constrain BSM physics.

the contrary, resummation effects are eventually needed to obtain reliable predictions in the tails of some kinematical distributions, for example in the invariant mass distribution of the W^+W^- pair [71].

As pointed out in Ref. [72], present experimental analyses for both ZZ and W^+W^- production assume the quark–antiquark ($q\bar{q}$) annihilation and loop-induced gluon fusion (gg) channels to be independent processes, although they mix in higher-order calculations through parton evolution. Already at NNLO there are diagrams that mix the two production mechanisms, thereby suggesting that a unified treatment would be desirable. Nevertheless, data are so far compared to *ad hoc* combinations of NNLO calculations for the quark annihilation channel and NLO corrections to the loop-induced gluon fusion channel, often by using K -factors (see e.g. Refs. [30, 31, 73, 74]). Ref. [72] made a decisive step for ZZ production by combining the NNLO calculation in the quark annihilation channel with the NLO calculation of the loop-induced gluon fusion channel. This is particularly important to perform consistent variations of the renormalisation and factorisation scales, which in turn allows us to obtain an estimate of perturbative uncertainties.

In this paper we take the same step for W^+W^- production, and supplement predictions for the NNLO QCD cross section with NLO QCD corrections to the loop-induced gg contribution. For the first time, we include also the (anti)quark–gluon (qg) channel entering the full NLO QCD corrections to the loop-induced channel. The combination of NNLO QCD contributions with NLO corrections to the loop-induced gluon fusion channel provides an estimate of the complete N³LO result and will be denoted by “nNNLO” in the following. This calculation constitutes the most advanced perturbative QCD prediction to date for the W^+W^- process. In order to reach the goal of percent-level theoretical uncertainties for W^+W^- production, QCD predictions must be combined with EW corrections at least at NLO, which has been achieved very recently in Ref. [45]. Our calculation, including the aforementioned EW corrections, will be made publicly available in an updated version of MATRIX [75]. In the following, we will discuss the details of the computation, analyse the effects of the newly computed corrections, and compare our best phenomenological predictions for differential observables in the fiducial phase space to ATLAS data at 13 TeV.

We consider the process

$$pp \rightarrow \ell^+ \ell'^- \nu_\ell \bar{\nu}_{\ell'} + X, \quad (1)$$

where the charged final-state leptons and the corresponding (anti)neutrinos have different flavours ($\ell \neq \ell'$). All the resonant and non-resonant Feynman diagrams contributing to this process are included, accounting for off-shell effects and spin correlations, and our calculation is fully differential in the momenta of the final-state leptons and the associated QCD radiation. The calculation is carried out by using the complex-mass scheme [76], without any resonance approximation. Our implementation can deal with any combination of (massless) leptonic flavours, $\ell, \ell' \in \{e, \mu\}$, and in order to compare against experimental data we focus on the process $pp \rightarrow \ell^+ \ell'^- \nu_\ell \bar{\nu}_{\ell'} + X$ with $\ell, \ell' = e$ or μ and $\ell \neq \ell'$. For the sake of brevity, we will denote this process as W^+W^- production in the following.

Representative LO diagrams are shown in Figure 1 (a–c). These are induced by $q\bar{q}$ annihilation and include t -channel W^+W^- topologies (panel a), s -channel W^+W^- topologies (panel b), and s -channel Drell–Yan-type topologies (panel c). Figure 1 (d), on the other hand, shows a gg diagram induced by a quark loop. The square of the corresponding amplitude enters at $\mathcal{O}(\alpha_s^2)$ and is part of the NNLO corrections. Furthermore, starting at NNLO, there is a mixing between quark

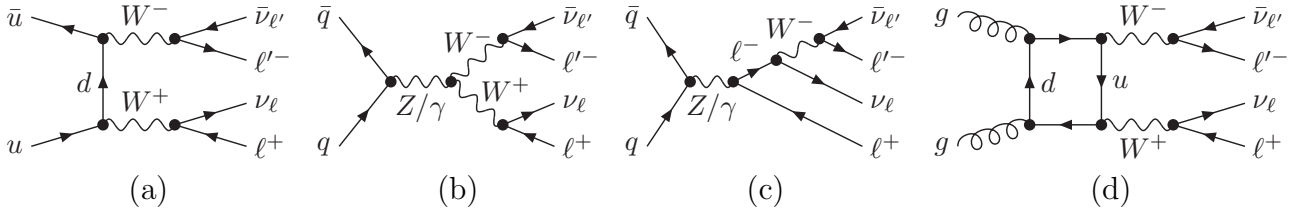


Figure 1: Sample Feynman diagrams contributing to W^+W^- production: (a-c) LO tree-level diagrams in the quark annihilation channel; (d) loop-induced diagram of the gluon fusion channel entering at $\mathcal{O}(\alpha_S^2)$.

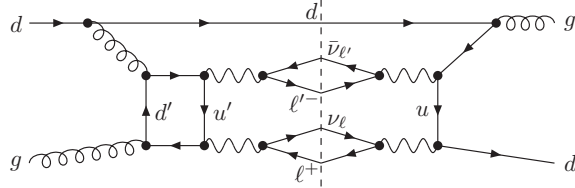


Figure 2: Example of NNLO interference between quark annihilation and loop-induced gluon fusion production mechanisms.

annihilation and gluon fusion contributions, see Figure 2 for example. Such mixing renders a distinction between the two production mechanisms ambiguous.

Nevertheless, the square of the loop-induced gg amplitude that enters at $\mathcal{O}(\alpha_S^2)$ is strongly enhanced by the large gluon luminosity, and it is formally only LO accurate. Consequently, the inclusion of the NLO corrections to this contribution becomes extremely important for obtaining a precise prediction for the W^+W^- cross section. Besides gg -initiated diagrams at $\mathcal{O}(\alpha_S^3)$ the NLO corrections entail also $q\bar{q}$ -initiated contributions.² The latter were neglected in the previous computation of the NLO corrections [61]. As we will see when presenting phenomenological results, the $q\bar{q}$ contributions can become quite relevant, in particular in cases where a jet veto is applied.

One should bear in mind that there are not only loop-induced contributions to the gg channel at $\mathcal{O}(\alpha_S^3)$, and that we only include contributions where both interfered amplitudes contain a closed fermion loop, see Figure 3 (a) for an example and Figure 3 (b) for a counterexample. At present it is not possible to consistently account for all the other contributions that would enter a complete next-to-next-to-next-to-leading-order (N^3 LO) calculation. For sufficiently inclusive observables, we expect the impact of the missing contributions at N^3 LO to be within the perturbative uncertainties estimated from NNLO scale variations. By contrast, NLO corrections to the loop-induced gg channel are known to exceed the uncertainties obtained through LO scale variations. Our partial N^3 LO results (nNNLO) therefore include all contributions up to $\mathcal{O}(\alpha_S^2)$, together with the complete NLO corrections to the loop-induced gluon fusion channel at $\mathcal{O}(\alpha_S^3)$. As such, besides providing the maximum information available at present in QCD perturbation theory for this process, our calculation provides a consistent estimate of the perturbative uncertainties through renormalization and factorization scale variations.

²There are also $q\bar{q}$ -initiated loop-induced contributions at $\mathcal{O}(\alpha_S^3)$. These are separately finite and completely negligible. Thus, we refrain from discussing them separately in the following, but include them in our numerical predictions.

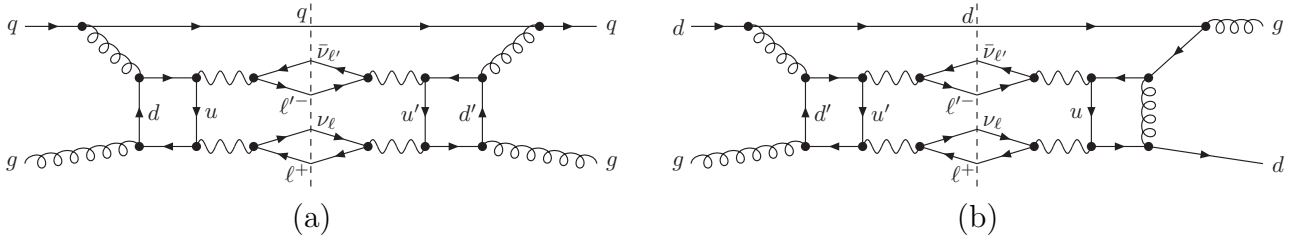


Figure 3: Examples of $N^3\text{LO}$ contributions in the qg channel, which are included (a) and excluded (b) in our NLO calculation for the loop-induced gluon fusion channel.

We perform our calculation in the computational framework MATRIX [75]. All tree-level and one-loop amplitudes are obtained with OPENLOOPS 2 [77, 78].³ For validation of the loop-induced contribution, we have employed the independent matrix-element generator RECOLA [82, 83], finding complete agreement. At two-loop level, we rely on the public C++ library VVAMP [84] that implements the $q\bar{q} \rightarrow VV'$ helicity amplitudes of Ref. [60] and the $gg \rightarrow VV'$ helicity amplitudes of Ref. [63]. The core of the MATRIX framework is the Monte Carlo program MUNICH⁴, which is capable of computing both NLO QCD and NLO EW [85, 86] corrections to arbitrary SM processes. To reach NNLO QCD accuracy, MATRIX uses a fully general implementation of the q_T -subtraction formalism [87]. The NLO calculation is performed by using the Catani–Seymour dipole-subtraction method [88, 89] and also with q_T subtraction [87], which provides an additional cross-check of our results. MATRIX has been employed in a large number of NNLO calculations for colour-singlet processes at hadron colliders [56, 57, 90–97]⁵, and it has been recently extended to heavy-quark production [98, 99]. MATRIX was also used for the NLO corrections to loop-induced ZZ production [72].

We present predictions for $pp \rightarrow \ell^+ \ell'^- \nu_\ell \bar{\nu}_{\ell'} + X$ production with $\ell, \ell' = e$ or μ and $\ell \neq \ell'$ at the LHC with $\sqrt{s} = 13$ TeV. For the EW parameters we employ the G_μ scheme and set $\alpha = \sqrt{2} G_F m_W^2 (1 - m_W^2/m_Z^2)/\pi$. We compute the EW mixing angle as $\cos\theta_W^2 = (m_W^2 - i\Gamma_W m_W)/(m_Z^2 - i\Gamma_Z m_Z)$ and use the complex-mass scheme [76] throughout. The input parameters are set to the PDG [100] values: $G_F = 1.16639 \times 10^{-5} \text{ GeV}^{-2}$, $m_W = 80.385 \text{ GeV}$, $\Gamma_W = 2.0854 \text{ GeV}$, $m_Z = 91.1876 \text{ GeV}$, $\Gamma_Z = 2.4952 \text{ GeV}$, $m_H = 125 \text{ GeV}$, and $\Gamma_H = 0.00407 \text{ GeV}$. The on-shell masses of the bottom and the top quark are $m_b = 4.92 \text{ GeV}$ and $m_t = 173.2 \text{ GeV}$, respectively, and a top width of $\Gamma_t = 1.44262 \text{ GeV}$ is used. The four-flavour scheme with $N_f = 4$ massless quark flavours and massive bottom and top quarks is used throughout. In this scheme contributions with massive bottom quarks in the final state are separately finite as they are regulated by the bottom-quark mass. We follow the prescription adopted in Refs. [56, 57] to avoid top-quark contamination: We drop all contributions with real bottom quarks in the final state to obtain a top-free W^+W^- cross section. Accordingly, we use the $N_f = 4$ sets of the NNPDF31 [101] parton distribution functions (PDFs) and choose the corresponding set for each perturbative order.⁶ The loop-induced gluon fusion contribution and also its NLO corrections are always computed

³OPENLOOPS 2 relies on its new on-the-fly tensor reduction [79] that guarantees numerical stability in the entire phase space, especially in the IR-singular regions. Within OPENLOOPS 2 scalar integrals from COLLIER [80] and ONELOOP [81] are used.

⁴MUNICH is the abbreviation of “MULTI-chaNNel Integrator at Swiss (CH) precision”—an automated parton level NLO generator by S. Kallweit. In preparation.

⁵It was also used in the NNLL+NNLO computation of Ref. [69], and in the NNLOPS computation of Ref. [70].

⁶At LO there is no $N_f = 4$ NNPDF31 PDF set available, so we use the corresponding NNPDF30 set [102].

definition of the fiducial volume for $pp \rightarrow \ell^+ \ell'^- \nu_\ell \bar{\nu}_{\ell'} + X$

$$\begin{aligned}
& p_{T,\ell/\ell'} > 27 \text{ GeV}, \quad |\eta_{\ell/\ell'}| < 2.5, \\
& m_{\ell\ell'} > 55 \text{ GeV}, \quad p_{T,\ell\ell'} > 30 \text{ GeV}, \quad p_{T,\text{miss}} > 20 \text{ GeV}, \\
& N_{\text{jets}} = 0 \text{ for anti-}k_T \text{ jets [103] with } R = 0.4, \quad p_{T,j} > 35 \text{ GeV}, \quad |\eta_j| < 4.5
\end{aligned}$$

Table 1: Phase-space definitions of the W^+W^- measurements by ATLAS at 13 TeV [32], with $\ell, \ell' = e$ or μ and $\ell \neq \ell'$.

with NNLO PDFs due to the lack of N³LO PDF sets. To improve the perturbative treatment in the tails of the kinematical distributions, we choose renormalization (μ_R) and factorization (μ_F) scales dynamically,

$$\mu_R = \mu_F = \mu_0 \equiv \frac{1}{2} \left(\sqrt{m_{\ell\nu_\ell}^2 + p_{T,\ell\nu_\ell}^2} + \sqrt{m_{\ell'\nu_{\ell'}}^2 + p_{T,\ell'\nu_{\ell'}}^2} \right), \quad (2)$$

where $m_{\ell\nu_\ell}$ and $p_{T,\ell\nu_\ell}$ ($m_{\ell'\nu_{\ell'}}$ and $p_{T,\ell'\nu_{\ell'}}$) are the invariant masses and the transverse momenta of the reconstructed W bosons. Residual uncertainties are estimated from customary 7-point variations, i.e. by varying μ_R and μ_F around the central scale μ_0 by a factor of two while respecting the constraint $0.5 \leq \mu_R/\mu_F \leq 2$.

Since the two-loop amplitudes including massive quarks are unknown to date, we employ the following approximation: The full dependence on the masses of top and bottom quarks is taken into account everywhere in the calculation, except for the two-loop virtual contributions. Since two-loop $q\bar{q} \rightarrow VV'$ diagrams with light fermion loops have a negligible impact, we expect also the massive quarks to induce subleading effects. For the two-loop $gg \rightarrow VV'$ contribution, on the other hand, we account for the heavy-quark masses approximately by reweighting the massless two-loop amplitude with the full LO one-loop amplitude including the massive quarks. Diagrams involving the Higgs boson are consistently included at each perturbative order, except for the two-loop contributions, where we employ the same approximation as for the massive top-quark loops.

We follow the ATLAS analysis at $\sqrt{s} = 13$ TeV of Ref. [32] and apply the selection cuts summarized in Table 1. The fiducial cuts involve standard requirements on the transverse momenta and pseudo-rapidities of the leptons, a lower invariant-mass cut and a lower cut on the transverse momentum of the lepton pair, as well as a minimum requirement on the missing transverse momentum. Most importantly, there is a jet veto as commonly applied in W^+W^- measurements to suppress the top-quark background. However, a particular feature of the fiducial setup of Ref. [32] as compared to previous W^+W^- analyses is the rather loose veto requirement which removes events with jets that have a p_T larger than $p_T^{\text{veto}} = 35$ GeV. Henceforth, our fixed-order calculation is expected to be reliable except in phase-space regions that involve scales significantly larger than the jet veto scale.

We briefly introduce our notation for the various contributions: $gg\text{LO}$ denotes the loop-induced gluon fusion channel contributing at $\mathcal{O}(\alpha_s^2)$, while the NNLO cross section in the quark annihilation channel (without the $gg\text{LO}$ contribution) is labelled $q\bar{q}\text{NNLO}$. $gg\text{NLO}$ refers to the complete NLO cross section of the loop-induced contribution, whereas $gg\text{NLO}_{gg}$ is its restriction to the gg -induced partonic channel. Hence, the difference between these two predictions corresponds to our newly

$\sqrt{s} = 13 \text{ TeV}$	jet veto	no jet veto	jet veto	no jet veto
	$\sigma \text{ [fb]}$		$\sigma/\sigma_{\text{NLO}} - 1$	
LO	$284.11(1)^{+5.5\%}_{-6.5\%}$	$284.11(1)^{+5.5\%}_{-6.5\%}$	-15.5%	-43.7%
NLO	$336.42(3)^{+1.6\%}_{-2.0\%}$	$504.36(3)^{+4.1\%}_{-3.3\%}$	$+0.\%$	$+0.\%$
$q\bar{q}$ NNLO	$336.8(2)^{+0.7\%}_{-0.5\%}$	$558.5(2)^{+2.1\%}_{-1.9\%}$	$+0.1\%$	$+10.7\%$
	$\sigma \text{ [fb]}$		$\sigma/\sigma_{\text{ggLO}} - 1$	
gg LO	$21.965(4)^{+25.7\%}_{-18.4\%}$	$21.965(4)^{+25.7\%}_{-18.4\%}$	$+0.\%$	$+0.\%$
gg NLO _{gg}	$31.68(6)^{+10.8\%}_{-10.6\%}$	$38.49(6)^{+15.9\%}_{-13.3\%}$	$+44.2\%$	$+75.2\%$
gg NLO	$28.79(6)^{+7.8\%}_{-9.1\%}$	$37.57(6)^{+15.3\%}_{-13.0\%}$	$+31.1\%$	$+71.0\%$
	$\sigma \text{ [fb]}$		$\sigma/\sigma_{\text{NLO}} - 1$	
NNLO	$358.7(2)^{+1.2\%}_{-0.9\%}$	$580.5(2)^{+2.9\%}_{-2.6\%}$	$+6.6\%$	$+15.1\%$
nNNLO	$365.6(2)^{+0.4\%}_{-0.6\%}$	$596.1(2)^{+2.8\%}_{-2.6\%}$	$+8.7\%$	$+18.2\%$
	$\sigma \text{ [fb]}$		$\sigma/\sigma_{\text{nNNLO}} - 1$	
nNNLO _{EW}	$354.3(2)^{+0.5\%}_{-0.8\%}$	$580.2(2)^{+2.7\%}_{-2.6\%}$	-3.1%	-2.7%

Table 2: Fiducial cross sections at different perturbative orders and relative impact on NLO and gg LO predictions, respectively. The quoted uncertainties correspond to scale variations as described in the text, and the numerical integration errors on the previous digit are stated in parentheses; for all (n)NNLO results, the latter include the uncertainty due the r_{cut} extrapolation [75].

computed contribution from the qg channels. As discussed before, our partial N³LO result is dubbed nNNLO, and it includes the full NNLO cross section supplemented by NLO corrections to the loop-induced gluon fusion contribution at $\mathcal{O}(\alpha_s^3)$.

In Table 2 we present cross sections at the various perturbative orders corresponding to the fiducial phase space defined in Table 1. Since the jet veto has a considerable impact on the structure of higher-order corrections, we show results in the same setup both *with* and *without* jet veto (i.e., inclusive over QCD radiation). The upper panel shows the QCD corrections to the quark annihilation channel, the second panel focusses on the loop-induced gluon fusion contribution up to $\mathcal{O}(\alpha_s^3)$, illustrating also the impact of the newly calculated qg channels, and the third panel compares the new best QCD prediction obtained in this paper, i.e. nNNLO, with the NNLO result. Our best fixed-order prediction is labelled nNNLO_{EW} and is reported in the last panel of Table 2. It is obtained by combining our nNNLO QCD result with NLO EW corrections according to the prescription of Ref. [45].⁷

⁷To be precise the nNNLO_{EW} prediction is obtained as follows. Only the EW corrections that can be uniquely assigned to the $q\bar{q}$ production channel are combined multiplicatively with the $q\bar{q}$ NNLO result, whereas the remaining EW corrections (photon-induced channels) as well as the gg NLO contribution are added. To account for the photon content of the proton, we use the NNPDF31_nnlo_as_0118_luxqed_nf_4 set [104] here, and we apply the same EW input and renormalization schemes as in Ref. [45]. By extending the notation of Ref. [45] this combined QCD–EW prediction could be also named nNNLO \times EW_{qq}.

The main conclusions that can be drawn from these results are the following:

- Cross sections with Born kinematics (LO and gg LO) are obviously not affected by cuts on QCD radiation. By contrast, the jet veto has a significant impact on higher-order QCD corrections, both in the quark-initiated channels and for the loop-induced gluon fusion contribution. In particular, the relative impact of the newly computed qg channel becomes quite sizeable with the jet veto. This can be understood as follows: Inclusively, the qg channel has a rather small and negative impact, since the negative $\overline{\text{MS}}$ mass factorization counterterm balances the positive contribution from the real radiation matrix elements. The jet veto acts only on the real radiation. Thus, it removes a positive contributions from the qg channel, rendering it more negative and increasing its relative impact. As we will discuss below, also for kinematical distributions the jet veto has quite a strong impact on the QCD corrections and the relative size of the qg channel. Without the jet veto radiative corrections are overall similar to those found for ZZ production in Ref. [72].
- The NLO (NNLO) corrections relative to LO (NLO) in the quark annihilation channel amount to +77.5% (+10.7%) without jet veto, and they are reduced to +18.4% (+0.1%) when the jet veto is applied.
- NLO corrections to the loop-induced gluon fusion channel are large: They are +71.0% in the case inclusive over QCD radiation and still +31.1% with the jet veto. The relative impact of the qg channel can be extracted from the difference between the gg NLO with gg NLO $_{qg}$ predictions. While in the inclusive case it reduces the gg NLO $_{qg}$ corrections to the loop-induced gluon fusion channel by only roughly 6%, this reduction increases to roughly 30% when the jet veto is applied.
- The NNLO QCD effects with a jet-veto amount to +6.6% with respect to NLO, and they are almost entirely due to the gg LO contribution, whereas the latter accounts for only about one third of the +15.1% NNLO corrections without jet veto. The impact of the NLO corrections to the loop-induced contribution is to increase the NNLO result by about 1.9% (2.7%) with (without) the jet veto. Excluding the qg channels would increase the nNNLO prediction with the jet veto by about 0.8%, while it has a subleading impact otherwise.
- NNLO and nNNLO predictions without jet veto are fully compatible within scale uncertainties. However, when the jet veto is applied, both at NNLO and at nNNLO the scale uncertainties are significantly reduced, and the two predictions are marginally compatible. Such strong reduction of scale uncertainties can be seen as a consequence of the improved convergence of the perturbative expansion, but it also suggests that scale uncertainties should not be fully trusted in this case as true perturbative uncertainties.
- Contributions stemming from intermediate Higgs boson exchange are included, but they are subdominant for the W^+W^- selection cuts under consideration. We find them to contribute only -0.3% to the fiducial W^+W^- cross section at nNNLO.
- Comparing our predictions to the measurement of the fiducial cross section reported in Ref. [32], $\sigma_{\text{fid}} = 379.1 \pm 5.0(\text{stat}) \pm 25.4(\text{syst}) \pm 8.0(\text{stat}) \text{ fb}$, we note that NNLO, nNNLO and nNNLO $_{\text{EW}}$ predictions are in agreement with the experimental result within one standard deviation. In general, as far as the central value is concerned, the positive effect of the gg NLO corrections slightly improves the agreement, while the EW corrections make the agreement slightly worse.

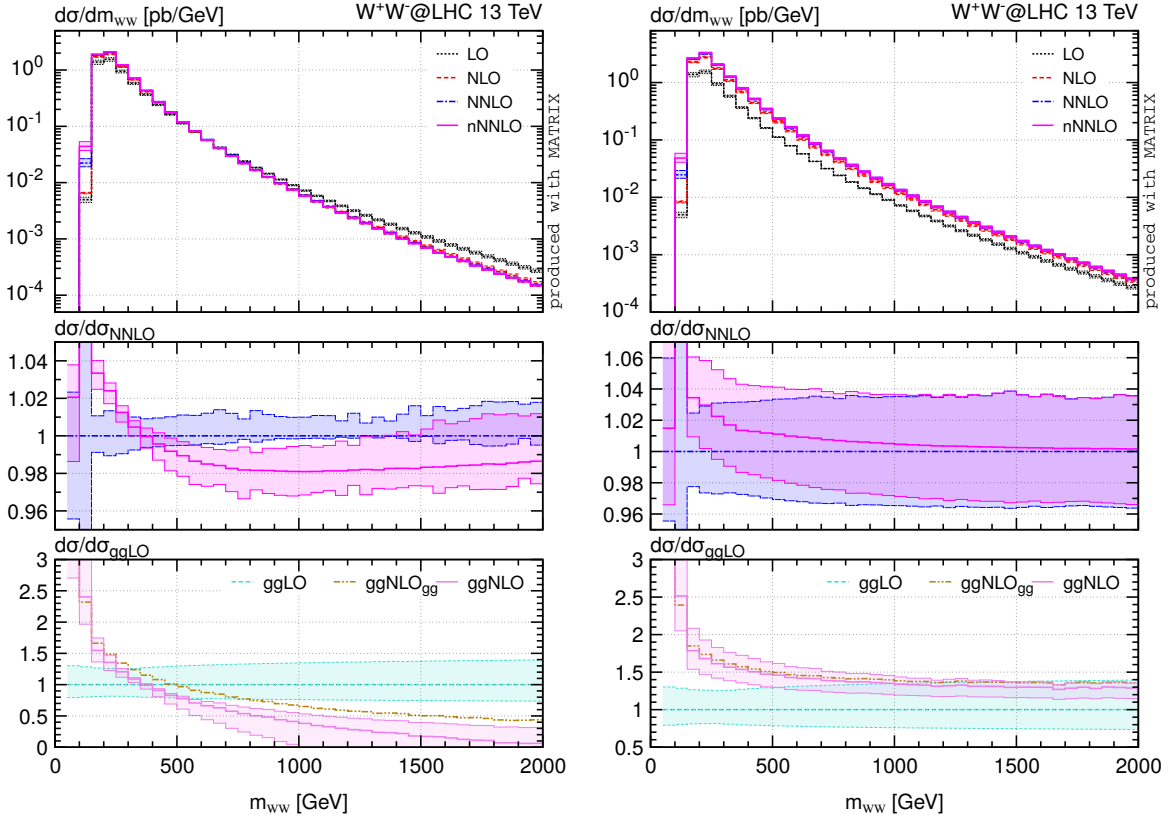


Figure 4: Invariant-mass distribution of the W^+W^- pair with jet veto (left) and without (right).

We now continue our presentation of phenomenological results by discussing kinematical distributions. In the following, all figures are organized according to the same pattern: The upper panel shows absolute cross sections at LO (black, dotted), NLO (red, dashed), NNLO (blue, dash-dotted) and nNNLO (magenta, solid). In the central panel the NNLO and nNNLO results including their scale uncertainty bands are normalised to the central NNLO prediction. The lower panel depicts the NLO/LO K -factors of the loop-induced gluon fusion contribution, with ($ggNLO$; pink, solid) and without ($ggNLO_{gg}$; brown, dash-double-dotted) the qg contribution. The results on the left are subject to the jet veto, whereas the ones on the right are inclusive over QCD radiation.

We first show the invariant-mass distribution of the W^+W^- pair (m_{WW}) in Figure 4. It is interesting to notice how the relative corrections are affected by the jet veto. Without jet veto (right panel) the loop-induced gluon fusion contribution at NLO is largest at small invariant masses ($\sim +3\%$ at the peak with respect to NNLO) and continuously decreases towards larger m_{WW} values, becoming negligible around 1 TeV. The $ggNLO$ correction is relatively flat (disregarding the region around the peak) and always positive, while the qg channel has a rather small impact, consistently with what we observed in Table 2. When the jet veto is applied (left panel), the shape of the NNLO prediction is significantly affected. The NLO corrections to the loop-induced contribution have a positive impact in the peak region ($\sim +3\%$ with respect to NNLO), but at larger invariant masses their effect turns negative, reaching $\sim -2\%$ in the TeV range. The $ggNLO$ K -factor strongly decreases as m_{WW} increases, and the impact of the qg channel is considerably large and negative at large m_{WW} .

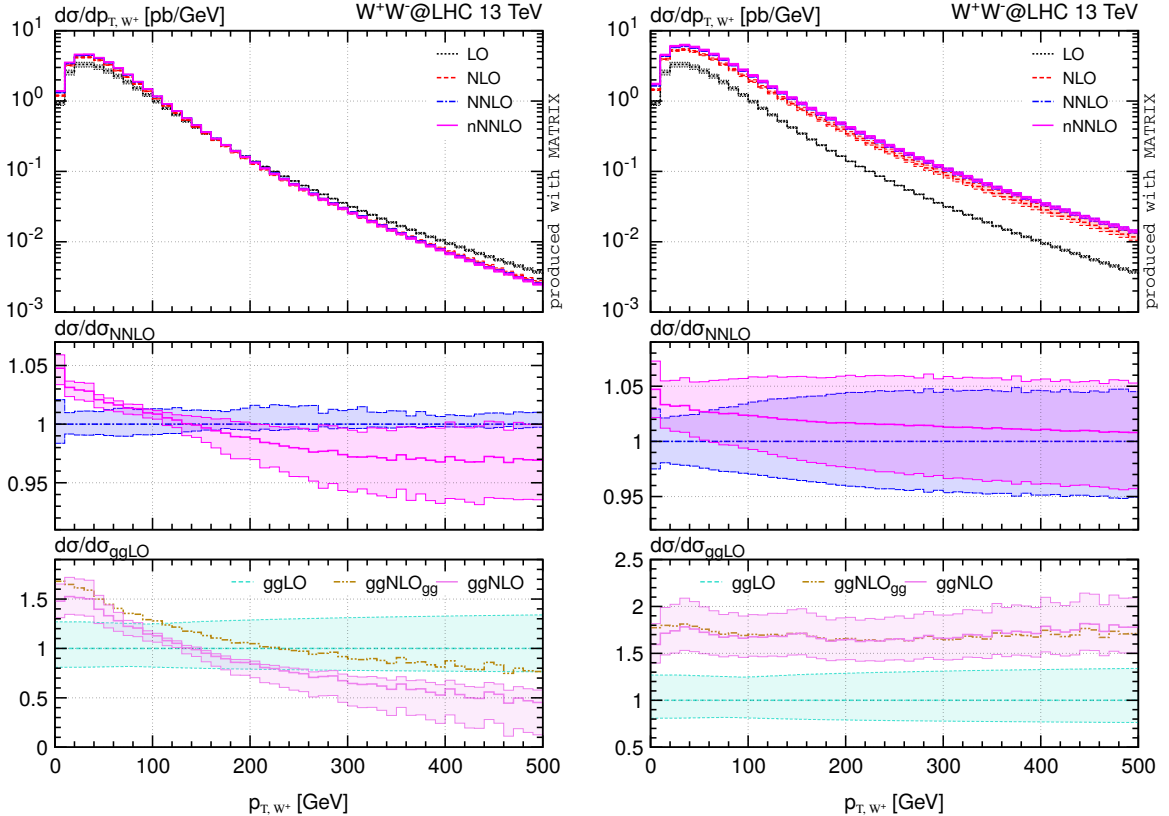


Figure 5: Transverse-momentum spectrum of the W boson with jet veto (left) and without (right).

This behaviour is not unexpected. As it is well known, at large m_{WW} the perturbative expansion is affected by large logarithmic contributions of the form $\alpha_s^n \ln^m m_{WW}/p_T^{\text{veto}}$, which would require an all-order resummation. Therefore, in the high- m_{WW} region fixed-order predictions become unreliable, and perturbative uncertainties are significantly larger than what can be inferred from customary scale variations.⁸ We note that the nNNLO uncertainty band widens in the tail of the m_{WW} distribution, becoming larger than the NNLO band. This effect is clearly driven by the interplay of the jet veto with the NLO corrections to the gg channel.

We find similar results for the transverse-momentum distribution of the reconstructed W^+ boson (p_{T,W^+}) in Figure 5; the distribution in p_{T,W^-} behaves similarly. Without the jet veto (right panel) the nNNLO corrections are positive at small transverse momenta, and they decrease as $p_{T,W}$ increases, but remain positive and small in the tail of the distribution. The gg NLO K -factor is almost completely flat and around +70%, with a minor impact of the qg channel. The small structure around $p_{T,W} \sim 150$ GeV is related to the massive-quark loop contributions. When the jet veto is applied (left panel) the nNNLO/NNLO ratio is about +5% at small transverse momenta and steadily decreases until it reaches about -3% for $p_{T,W} \gtrsim 300$ GeV. The gg NLO correction is positive at small transverse momenta and it significantly decreases as $p_{T,W}$ increases, with a considerable effect coming from the qg channel.

⁸Note that such pathological behaviour could be avoided by employing a dynamic jet-veto definition, as suggested for instance in Refs. [44, 45] to tame giant QCD K -factors in the high-energy tails of kinematical distributions.

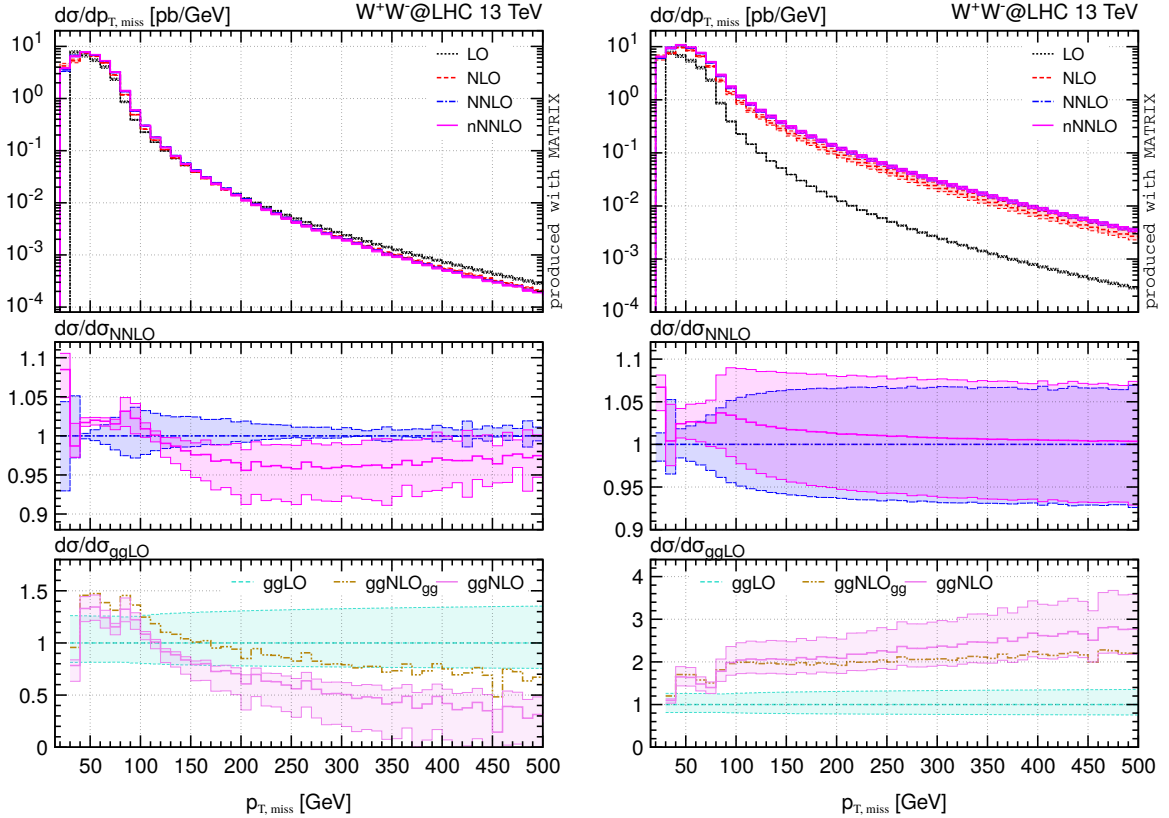


Figure 6: Missing transverse-momentum distribution with jet veto (left) and without (right).

In Figure 6 we show the distribution in the missing transverse momentum ($p_{T,\text{miss}}$) computed from the vectorial sum of the neutrino momenta. The pattern of the corrections with and without jet veto is rather similar to the two distributions considered before. We thus only discuss one peculiar additional feature, namely the kink around $p_{T,\text{miss}} \sim m_W$, which is visible in all the predictions. We also note that the size of the uncertainty bands for $p_{T,\text{miss}} > m_W$ clearly increases. Such effect is due to the fact that at LO the two neutrinos are back-to-back with the leptons, and therefore values of $p_{T,\text{miss}}$ larger than m_W are strongly disfavoured as they require at least one of the W bosons to go off-shell. This can be seen also from the quickly decreasing LO result for $p_{T,\text{miss}} > m_W$ in the case in which no jet veto is applied. At NLO the neutrinos can recoil against the additional jet, and this region receives a large correction. Hence, the accuracy is effectively reduced by one order here, which explains also the enlarged uncertainty bands. The impact of the NLO corrections in the quark annihilation channel without jet veto is indeed huge, with K -factors of $\mathcal{O}(10)$ in the high- $p_{T,\text{miss}}$ region.

We finally perform a comparison of our nNNLO predictions to the ATLAS data of Ref. [32] in Figure 7. On top of the pure QCD predictions, we also show the best available fixed-order result nNNLO_{EW} (green, long-dashed), which was introduced in Table 2 and includes also the EW effects calculated in Ref. [45]. In general, the NLO corrections to the loop-induced contribution slightly improve the agreement with the data, especially when the nNNLO prediction has a different shape compared to NNLO, i.e. for the distributions in the transverse momentum of the leading lepton (p_{T,ℓ_1} , upper left plot), the invariant mass of the lepton pair (m_{WW} , upper central plot)

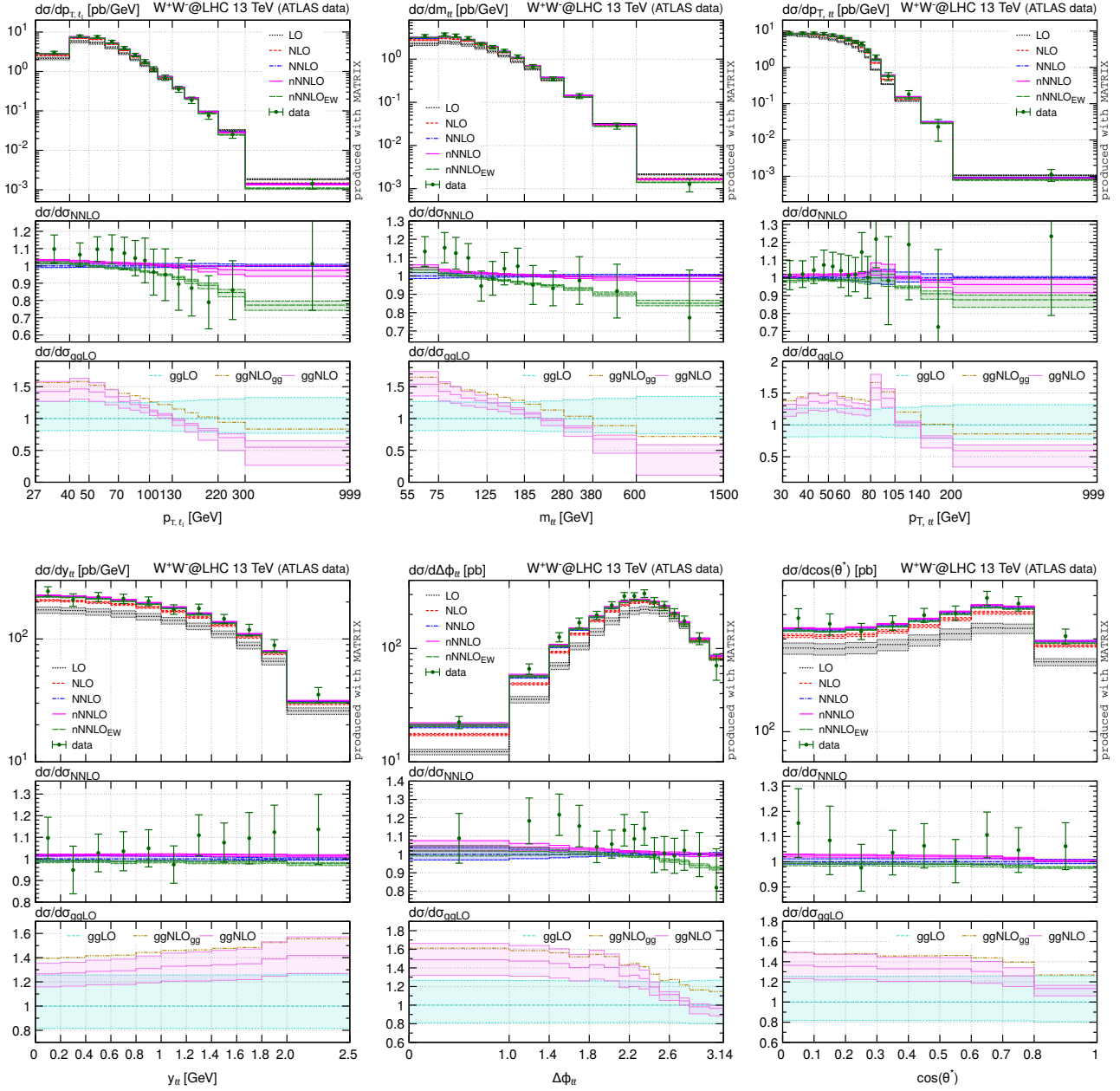


Figure 7: Differential distributions in the fiducial phase space selections of Table 1 compared to ATLAS 13 TeV data [32]; top left: leading-lepton transverse-momentum distribution; top center: lepton-pair invariant-mass distribution; top right: lepton-pair transverse-momentum distribution; bottom left: lepton-pair rapidity distribution; bottom center: azimuthal distance between leptons; bottom right: distribution in the variable $|\cos \theta^*| = |\tanh(\Delta\eta_{\ell\ell}/2)|$.

and the transverse momentum of the dilepton system ($p_{T,\ell\ell}$, upper right plot), as well as for the distribution in the azimuthal angle between the leptons ($\Delta\phi_{\ell\ell}$, lower central plot). The experimental uncertainties, however, are still too large to draw firm conclusions. In the tails of the p_{T,ℓ_1} , m_{WW} and $p_{T,\ell\ell}$ distributions, the negative effects of the EW Sudakov logarithms are clearly more pronounced than those of the gg NLO corrections. For the rapidity distribution of the lepton pair ($y_{\ell\ell}$, lower left plot) and the distribution in $|\cos\theta^*| = |\tanh(\Delta\eta_{\ell\ell}/2)|$ (lower right plot), the gg NLO corrections are largely flat with respect to the NNLO result, and the better agreement of the nNNLO distribution with data is only due to the normalization, which was already found for the fiducial cross section in Table 2.

We have calculated NLO QCD radiative corrections to the loop-induced gluon fusion contribution in W^+W^- production at the LHC. Our predictions include, for the first time, also (anti)quark–gluon partonic channels. By combining these results with the NNLO QCD prediction for quark annihilation we have obtained an estimate of the full N³LO cross section, denoted by nNNLO, which represents the most advanced QCD prediction available to date for this process. By considering the full leptonic signature $pp \rightarrow \ell^+\ell'^-\nu_{\ell}\bar{\nu}_{\ell'} + X$, we consistently account for off-shell effects, spin correlations and interferences. We have presented phenomenological results for the fiducial cross section and distributions applying the selection criteria used in the ATLAS measurement at $\sqrt{s} = 13$ TeV, which include a jet veto. This jet veto, which is customarily applied to suppress the top quark background, has a significant impact on the behaviour of radiative corrections. In particular the shapes of important distributions are modified by NLO corrections to the loop-induced gluon fusion contribution. Our results are in good agreement with the experimental data, which, however, have still large uncertainties. Our calculation has been implemented in the parton-level Monte Carlo program MATRIX and will be made available in a forthcoming version of the code. Together with the combination of EW corrections (already included in the comparison with experimental data here), presented in parallel to this work in Ref. [45], our results will boost the precision in physics studies based on the W^+W^- signature at the LHC and future hadron colliders.

Acknowledgements. We thank Fabrizio Caola, Raul Röntschi and Lorenzo Tancredi for helpful discussions. We are particularly indebted to Jonas Lindert and Federico Buccioni for useful correspondence, and for making private OPENLOOPS amplitudes for the loop-induced channel available to us. Moreover, we want to thank Jean-Nicolas Lang for his help on interfacing RECOLA and validating the OPENLOOPS results. This work is supported in part by the Swiss National Science Foundation (SNF) under contracts CRSII2-141847 and 200020-169041. The work of MW was supported by the ERC Consolidator Grant 614577 HICCUP, and that of SK by the ERC Starting Grant 714788 REINVENT.

References

- [1] G. Aad *et al.* (ATLAS), Phys. Rev. **D87**, 112001 (2013), arXiv:1210.2979 [hep-ex].
- [2] S. Chatrchyan *et al.* (CMS), Eur. Phys. J. **C73**, 2610 (2013), arXiv:1306.1126 [hep-ex].
- [3] J. Wang (ATLAS, D0, CDF, CMS), Int. J. Mod. Phys. Conf. Ser. **31**, 1460279 (2014), arXiv:1403.1415 [hep-ex].
- [4] V. Khachatryan *et al.* (CMS), Eur. Phys. J. **C76**, 401 (2016), arXiv:1507.03268 [hep-ex].
- [5] G. Aad *et al.* (ATLAS), JHEP **09**, 029 (2016), arXiv:1603.01702 [hep-ex].
- [6] C. Frye, M. Freytsis, J. Scholtz and M. J. Strassler, JHEP **03**, 171 (2016), arXiv:1510.08451 [hep-ph].
- [7] A. Butter, O. J. P. Éboli, J. Gonzalez-Fraile, M. C. Gonzalez-Garcia, T. Plehn and M. Rauch, JHEP **07**, 152 (2016), arXiv:1604.03105 [hep-ph].
- [8] Z. Zhang, Phys. Rev. Lett. **118**, 011803 (2017), arXiv:1610.01618 [hep-ph].
- [9] D. R. Green, P. Meade and M.-A. Pleier, Rev. Mod. Phys. **89**, 035008 (2017), arXiv:1610.07572 [hep-ex].
- [10] J. Baglio, S. Dawson and I. M. Lewis, Phys. Rev. **D96**, 073003 (2017), arXiv:1708.03332 [hep-ph].
- [11] A. Falkowski, M. Gonzalez-Alonso, A. Greljo, D. Marzocca and M. Son, JHEP **02**, 115 (2017), arXiv:1609.06312 [hep-ph].
- [12] G. Panico, F. Riva and A. Wulzer, Phys. Lett. **B776**, 473 (2018), arXiv:1708.07823 [hep-ph].
- [13] R. Franceschini, G. Panico, A. Pomarol, F. Riva and A. Wulzer, JHEP **02**, 111 (2018), arXiv:1712.01310 [hep-ph].
- [14] D. Liu and L.-T. Wang, Phys. Rev. **D99**, 055001 (2019), arXiv:1804.08688 [hep-ph].
- [15] G. Aad *et al.* (ATLAS), Phys. Lett. **B716**, 1 (2012), arXiv:1207.7214 [hep-ex].
- [16] S. Chatrchyan *et al.* (CMS), Phys. Lett. **B716**, 30 (2012), arXiv:1207.7235 [hep-ex].
- [17] G. Aad *et al.* (ATLAS), Phys. Lett. **B726**, 120 (2013), arXiv:1307.1432 [hep-ex].
- [18] G. Aad *et al.* (ATLAS), Phys. Rev. **D92**, 012006 (2015), arXiv:1412.2641 [hep-ex].
- [19] G. Aad *et al.* (ATLAS), Eur. Phys. J. **C75**, 476 (2015), [Erratum: Eur. Phys. J. **C76**, no.3, 152 (2016)], arXiv:1506.05669 [hep-ex].
- [20] G. Aad *et al.* (ATLAS), JHEP **08**, 104 (2016), arXiv:1604.02997 [hep-ex].
- [21] M. Aaboud *et al.* (ATLAS), Phys. Lett. **B786**, 223 (2018), arXiv:1808.01191 [hep-ex].
- [22] S. Chatrchyan *et al.* (CMS), Phys. Rev. **D89**, 092007 (2014), arXiv:1312.5353 [hep-ex].

- [23] S. Chatrchyan et al. (CMS), JHEP **01**, 096 (2014), arXiv:1312.1129 [hep-ex].
- [24] S. Chatrchyan et al. (CMS), JHEP **06**, 081 (2013), arXiv:1303.4571 [hep-ex].
- [25] V. Khachatryan et al. (CMS), Phys. Rev. **D92**, 072010 (2015), arXiv:1507.06656 [hep-ex].
- [26] G. Aad et al. (ATLAS, CMS), JHEP **08**, 045 (2016), arXiv:1606.02266 [hep-ex].
- [27] V. Khachatryan et al. (CMS), JHEP **03**, 032 (2017), arXiv:1606.01522 [hep-ex].
- [28] T. Aaltonen et al. (CDF), Phys. Rev. Lett. **104**, 201801 (2010), arXiv:0912.4500 [hep-ex].
- [29] V. M. Abazov et al. (D0), Phys. Rev. Lett. **108**, 181803 (2012), arXiv:1112.0536 [hep-ex].
- [30] M. Aaboud et al. (ATLAS), Phys. Lett. **B773**, 354 (2017), arXiv:1702.04519 [hep-ex].
- [31] C. Collaboration (CMS), CMS-PAS-SMP-16-006.
- [32] M. Aaboud et al. (ATLAS), Eur. Phys. J. **C79**, 884 (2019), arXiv:1905.04242 [hep-ex].
- [33] R. Brown and K. Mikaelian, Phys. Rev. **D19**, 922 (1979).
- [34] J. Ohnemus, Phys. Rev. **D44**, 1403 (1991).
- [35] S. Frixione, Nucl. Phys. **B410**, 280 (1993).
- [36] J. M. Campbell and R. K. Ellis, Phys. Rev. **D60**, 113006 (1999), hep-ph/9905386.
- [37] L. J. Dixon, Z. Kunszt and A. Signer, Phys. Rev. **D60**, 114037 (1999), hep-ph/9907305.
- [38] L. J. Dixon, Z. Kunszt and A. Signer, Nucl. Phys. **B531**, 3 (1998), hep-ph/9803250.
- [39] J. M. Campbell, R. K. Ellis and C. Williams, JHEP **1107**, 018 (2011), arXiv:1105.0020 [hep-ph].
- [40] A. Bierweiler, T. Kasprzik, J. H. Kühn and S. Uccirati, JHEP **1211**, 093 (2012), arXiv:1208.3147 [hep-ph].
- [41] J. Baglio, L. D. Ninh and M. M. Weber, Phys. Rev. **D88**, 113005 (2013), arXiv:1307.4331 [hep-ph].
- [42] M. Billoni, S. Dittmaier, B. Jäger and C. Speckner, JHEP **1312**, 043 (2013), arXiv:1310.1564 [hep-ph].
- [43] B. Biedermann, M. Billoni, A. Denner, S. Dittmaier, L. Hofer, B. Jäger and L. Salfelder, JHEP **06**, 065 (2016), arXiv:1605.03419 [hep-ph].
- [44] S. Kallweit, J. M. Lindert, S. Pozzorini and M. Schönherr, JHEP **11**, 120 (2017), arXiv:1705.00598 [hep-ph].
- [45] S. Kallweit, M. Grazzini, J. M. Lindert, S. Pozzorini and M. Wiesemann, (2019), arXiv:1912.00068 [hep-ph].
- [46] E. W. N. Glover and J. J. van der Bij, Nucl. Phys. **B321**, 561 (1989).

- [47] D. A. Dicus, C. Kao and W. W. Repko, Phys. Rev. **D36**, 1570 (1987).
- [48] T. Matsuura and J. van der Bij, Z. Phys. **C51**, 259 (1991).
- [49] C. Zecher, T. Matsuura and J. van der Bij, Z. Phys. **C64**, 219 (1994), hep-ph/9404295.
- [50] T. Binoth, N. Kauer and P. Mertsch, Proceedings **DIS 2008**, 142 (2008), arXiv:0807.0024 [hep-ph].
- [51] N. Kauer, JHEP **12**, 082 (2013), arXiv:1310.7011 [hep-ph].
- [52] F. Cascioli, S. Höche, F. Krauss, P. Maierhöfer, S. Pozzorini and F. Siegert, JHEP **1401**, 046 (2014), arXiv:1309.0500 [hep-ph].
- [53] J. M. Campbell, R. K. Ellis and C. Williams, JHEP **04**, 060 (2014), arXiv:1311.3589 [hep-ph].
- [54] J. M. Campbell, R. K. Ellis and C. Williams, PoS **LL2014**, 008 (2014), arXiv:1408.1723 [hep-ph].
- [55] N. Kauer, C. O'Brien and E. Vryonidou, JHEP **10**, 074 (2015), arXiv:1506.01694 [hep-ph].
- [56] T. Gehrmann, M. Grazzini, S. Kallweit, P. Maierhöfer, A. von Manteuffel, S. Pozzorini, D. Rathlev and L. Tancredi, Phys. Rev. Lett. **113**, 212001 (2014), arXiv:1408.5243 [hep-ph].
- [57] M. Grazzini, S. Kallweit, S. Pozzorini, D. Rathlev and M. Wiesemann, JHEP **08**, 140 (2016), arXiv:1605.02716 [hep-ph].
- [58] T. Gehrmann, A. von Manteuffel, L. Tancredi and E. Weihs, JHEP **1406**, 032 (2014), arXiv:1404.4853 [hep-ph].
- [59] F. Caola, J. M. Henn, K. Melnikov, A. V. Smirnov and V. A. Smirnov, JHEP **1411**, 041 (2014), arXiv:1408.6409 [hep-ph].
- [60] T. Gehrmann, A. von Manteuffel and L. Tancredi, JHEP **09**, 128 (2015), arXiv:1503.04812 [hep-ph].
- [61] F. Caola, K. Melnikov, R. Rötsch and L. Tancredi, Phys. Lett. **B754**, 275 (2016), arXiv:1511.08617 [hep-ph].
- [62] F. Caola, J. M. Henn, K. Melnikov, A. V. Smirnov and V. A. Smirnov, JHEP **1506**, 129 (2015), arXiv:1503.08759 [hep-ph].
- [63] A. von Manteuffel and L. Tancredi, JHEP **1506**, 197 (2015), arXiv:1503.08835 [hep-ph].
- [64] P. Jaiswal and T. Okui, Phys. Rev. **D90**, 073009 (2014), arXiv:1407.4537 [hep-ph].
- [65] P. Meade, H. Ramani and M. Zeng, Phys. Rev. **D90**, 114006 (2014), arXiv:1407.4481 [hep-ph].
- [66] T. Becher, R. Frederix, M. Neubert and L. Rothen, Eur.Phys.J. **C75**, 154 (2015), arXiv:1412.8408 [hep-ph].
- [67] P. F. Monni and G. Zanderighi, JHEP **1505**, 013 (2015), arXiv:1410.4745 [hep-ph].

- [68] S. Dawson, P. Jaiswal, Y. Li, H. Ramani and M. Zeng, *Phys. Rev.* **D94**, 114014 (2016), arXiv:1606.01034 [hep-ph].
- [69] M. Grazzini, S. Kallweit, D. Rathlev and M. Wiesemann, *JHEP* **08**, 154 (2015), arXiv:1507.02565 [hep-ph].
- [70] E. Re, M. Wiesemann and G. Zanderighi, *JHEP* **12**, 121 (2018), arXiv:1805.09857 [hep-ph].
- [71] L. Arpino, A. Banfi, S. Jäger and N. Kauer, *JHEP* **08**, 076 (2019), arXiv:1905.06646 [hep-ph].
- [72] M. Grazzini, S. Kallweit, M. Wiesemann and J. Y. Yook, *JHEP* **03**, 070 (2019), arXiv:1811.09593 [hep-ph].
- [73] M. Aaboud et al. (ATLAS), *Phys. Rev.* **D97**, 032005 (2018), arXiv:1709.07703 [hep-ex].
- [74] A. M. Sirunyan et al. (CMS), *Eur. Phys. J.* **C78**, 165 (2018), arXiv:1709.08601 [hep-ex].
- [75] M. Grazzini, S. Kallweit and M. Wiesemann, *Eur. Phys. J.* **C78**, 537 (2018), arXiv:1711.06631 [hep-ph].
- [76] A. Denner, S. Dittmaier, M. Roth and L. H. Wieders, *Nucl. Phys.* **B724**, 247 (2005), [Erratum: *Nucl. Phys.* B854, 504 (2012)], hep-ph/0505042.
- [77] F. Cascioli, P. Maierhöfer and S. Pozzorini, *Phys. Rev. Lett.* **108**, 111601 (2012), arXiv:1111.5206 [hep-ph].
- [78] F. Buccioni, J.-N. Lang, J. M. Lindert, P. Maierhöfer, S. Pozzorini, H. Zhang and M. F. Zoller, *Eur. Phys. J.* **C79**, 866 (2019), arXiv:1907.13071 [hep-ph].
- [79] F. Buccioni, S. Pozzorini and M. Zoller, *Eur. Phys. J.* **C78**, 70 (2018), arXiv:1710.11452 [hep-ph].
- [80] A. Denner, S. Dittmaier and L. Hofer, *Comput. Phys. Commun.* **212**, 220 (2017), arXiv:1604.06792 [hep-ph].
- [81] A. van Hameren, *Comput. Phys. Commun.* **182**, 2427 (2011), arXiv:1007.4716 [hep-ph].
- [82] S. Actis, A. Denner, L. Hofer, J.-N. Lang, A. Scharf and S. Uccirati, *Comput. Phys. Commun.* **214**, 140 (2017), arXiv:1605.01090 [hep-ph].
- [83] A. Denner, J.-N. Lang and S. Uccirati, *Comput. Phys. Commun.* **224**, 346 (2018), arXiv:1711.07388 [hep-ph].
- [84] The VVAMP project, by T. Gehrmann, A. von Manteuffel, and L. Tancredi, is publicly available at <http://vvamp.hepforge.org>.
- [85] S. Kallweit, J. M. Lindert, P. Maierhöfer, S. Pozzorini and M. Schönherr, *JHEP* **04**, 012 (2015), arXiv:1412.5157 [hep-ph].
- [86] S. Kallweit, J. M. Lindert, P. Maierhöfer, S. Pozzorini and M. Schönherr, *JHEP* **04**, 021 (2016), arXiv:1511.08692 [hep-ph].
- [87] S. Catani and M. Grazzini, *Phys. Rev. Lett.* **98**, 222002 (2007), hep-ph/0703012.

- [88] S. Catani and M. Seymour, Phys. Lett. **B378**, 287 (1996), hep-ph/9602277.
- [89] S. Catani and M. Seymour, Nucl. Phys. **B485**, 291 (1997), hep-ph/9605323.
- [90] M. Grazzini, S. Kallweit, D. Rathlev and A. Torre, Phys. Lett. **B731**, 204 (2014), arXiv:1309.7000 [hep-ph].
- [91] M. Grazzini, S. Kallweit and D. Rathlev, JHEP **07**, 085 (2015), arXiv:1504.01330 [hep-ph].
- [92] F. Cascioli, T. Gehrmann, M. Grazzini, S. Kallweit, P. Maierhöfer, A. von Manteuffel, S. Pozzorini, D. Rathlev, L. Tancredi and E. Weihs, Phys. Lett. **B735**, 311 (2014), arXiv:1405.2219 [hep-ph].
- [93] M. Grazzini, S. Kallweit and D. Rathlev, Phys. Lett. **B750**, 407 (2015), arXiv:1507.06257 [hep-ph].
- [94] M. Grazzini, S. Kallweit, D. Rathlev and M. Wiesemann, Phys. Lett. **B761**, 179 (2016), arXiv:1604.08576 [hep-ph].
- [95] M. Grazzini, S. Kallweit, D. Rathlev and M. Wiesemann, JHEP **05**, 139 (2017), arXiv:1703.09065 [hep-ph].
- [96] D. de Florian, M. Grazzini, C. Hanga, S. Kallweit, J. M. Lindert, P. Maierhöfer, J. Mazzitelli and D. Rathlev, JHEP **09**, 151 (2016), arXiv:1606.09519 [hep-ph].
- [97] M. Grazzini, G. Heinrich, S. Jones, S. Kallweit, M. Kerner, J. M. Lindert and J. Mazzitelli, JHEP **05**, 059 (2018), arXiv:1803.02463 [hep-ph].
- [98] S. Catani, S. Devoto, M. Grazzini, S. Kallweit, J. Mazzitelli and H. Sargsyan, Phys. Rev. **D99**, 051501 (2019), arXiv:1901.04005 [hep-ph].
- [99] S. Catani, S. Devoto, M. Grazzini, S. Kallweit and J. Mazzitelli, JHEP **07**, 100 (2019), arXiv:1906.06535 [hep-ph].
- [100] C. Patrignani et al. (Particle Data Group), Chin. Phys. **C40**, 100001 (2016).
- [101] R. D. Ball et al. (NNPDF), Eur. Phys. J. **C77**, 663 (2017), arXiv:1706.00428 [hep-ph].
- [102] R. D. Ball et al. (NNPDF), JHEP **1504**, 040 (2015), arXiv:1410.8849 [hep-ph].
- [103] M. Cacciari, G. P. Salam and G. Soyez, JHEP **0804**, 063 (2008), arXiv:0802.1189 [hep-ph].
- [104] V. Bertone, S. Carrazza, N. P. Hartland and J. Rojo (NNPDF), SciPost Phys. **5**, 008 (2018), arXiv:1712.07053 [hep-ph].